3-8-2010

Effect of carbon addition on the single crystalline magnetostriction of Fe-X (X = Al and Ga) alloys

Mianliang Huang
Iowa State University

Yingzhou Du
Iowa State University, yzdu@iastate.edu

Robert J. McQueeney
Iowa State University, mcqueeney@ameslab.gov

Thomas A. Lograsso
Iowa State University, lograsso@ameslab.gov

Effect of carbon addition on the single crystalline magnetostriction of Fe-X (X = Al and Ga) alloys

Abstract
The effect of carbon addition on the magnetostriction of Fe–Ga and Fe–Al alloys was investigated and is summarized in this study. It was found that the addition of carbon generally increased the magnetostriction over binary alloys of Fe–Ga and Fe–Al systems. The formation of carbide in the Fe–Ga–C alloys with a composition near $D0_3$ phase region decreased the magnetostriction drastically. Fe–Al–C and Fe–Ga–C alloys responded differently to thermal treatments; the magnetostriction in the quenched Fe–Al–C alloys is equal to or slightly lower than that of the slow cooled as is observed in binary Fe–Al alloy; in contrast, the magnetostriction is generally higher in quenched Fe–Ga–C alloys than slow cooled condition, consistent with the behavior of binary alloys of Fe–Ga. A significant increase in magnetostriction between 25% and 165% depending on the phase region in Fe–Ga–C alloys by quenching was observed in the A2+$D0_3$ two-phase region and $D0_3$ single phase region.

Keywords
Physics and Astronomy, IPRT, alloying additions, aluminium alloys, carbon, gallium alloys, iron alloys, magnetostriction, quenching (thermal)

Disciplines
Condensed Matter Physics | Metallurgy

Comments
The following article appeared in *Journal of Applied Physics* 107 (2010): 053520 and may be found at http://dx.doi.org/10.1063/1.3311884.

AIP | Journal of Applied Physics

Effect of carbon addition on the single crystalline magnetostriction of Fe-X (X = Al and Ga) alloys

Mianliang Huang, Yingzhou Du, Robert J. McQueeney, and Thomas A. Lograsso

Citation: J. Appl. Phys. **107**, 053520 (2010); doi: 10.1063/1.3311884
View online: http://dx.doi.org/10.1063/1.3311884
View Table of Contents: http://jap.aip.org/resource/1/JAPIAU/v107/i5
Published by the AIP Publishing LLC.

Effect of carbon addition on the single crystalline magnetostriction of Fe-X (X=Al and Ga) alloys

Mianliang Huang,[1,a)] Yingzhou Du,[2] Robert J. McQueeney,[2] and Thomas A. Lograsso[1]
[1]*Institute for Physical Research and Technology, Iowa State University, Ames, Iowa 50011, USA*
[2]*Department of Physics and Astronomy, Iowa State University, Ames, Iowa 50011, USA*

(Received 11 August 2009; accepted 18 January 2010; published online 8 March 2010)

The effect of carbon addition on the magnetostriction of Fe–Ga and Fe–Al alloys was investigated and is summarized in this study. It was found that the addition of carbon generally increased the magnetostriction over binary alloys of Fe–Ga and Fe–Al systems. The formation of carbide in the Fe–Ga–C alloys with a composition near $D0_3$ phase region decreased the magnetostriction drastically. Fe–Al–C and Fe–Ga–C alloys responded differently to thermal treatments; the magnetostriction in the quenched Fe–Al–C alloys is equal to or slightly lower than that of the slow cooled as is observed in binary Fe–Al alloy; in contrast, the magnetostriction is generally higher in quenched Fe–Ga–C alloys than slow cooled condition, consistent with the behavior of binary alloys of Fe–Ga. A significant increase in magnetostriction between 25% and 165% depending on the phase region in Fe–Ga–C alloys by quenching was observed in the $A2+D0_3$ two-phase region and $D0_3$ single phase region. © *2010 American Institute of Physics*. [doi:10.1063/1.3311884]

I. INTRODUCTION

Recently, Clark and his collaborators[1–7] discovered that Fe–Ga alloys possess the highest single crystalline magnetostrictive strain for a binary alloy (approximately ten times that of pure Fe) and unlike other magnetostrictive alloys, retain significant ductility. The high magnetostriction (MS) combined with the good mechanical properties makes Fe–Ga alloys a promising material with applications in actuator, sensor, and other devices. The exploration of ternary Fe-based alloys has been carried out to search alloys with a higher MS as well to improve mechanical properties and/or corrosion resistance.[8,9] Previous work[9] indicates that additions of transition metal elements at levels greater than 2 at. % reduce the saturation MS of single crystalline Fe–Ga samples. The decrease in MS in ternary Fe–Ga alloys containing transition metal elements is due to the increased stability of the $D0_3$ structure.[9,10] In contrast, it has been found that small amounts of C additions in Fe–Ga alloys can increase the tetragonal MS λ_{100} by approximately 10%–30% in the composition range of ~5–22 at. % Ga.[8,9] Further microstructural characterization found that carbon additions extended the single phase body-centered-cubic (bcc) α-Fe phase region to higher Ga contents. Extension of the α phase region in Fe–Ga beyond the binary solubility limit leads to even larger values of λ_{100} than previously reported.

Trends in the tetragonal MS of Fe–Ga alloys closely follow the phase relations in the binary metastable phase diagram.[11,12] Our previous studies mainly focused on the effect of carbon addition into Fe–Ga alloys with Ga content up to ~23 at. %, corresponding to the A2 and $A2+D0_3$ phase regions.[8,11] In this study, we extended our study on carbon addition into Fe–Ga alloys over a composition range of ~25–30 at. % Ga, where the dominant phase is $D0_3$, and the added carbon may behave differently from that in the other phase regions.

The stable Fe–Al (Ref. 13) phase diagram is similar to the metastable Fe–Ga (Ref. 12) phase diagram at room temperature, i.e., there are phase regions that consist of A2, $A2+D0_3$, and $D0_3$ at compositions of up to 40 at. %. Therefore, it is not unexpected that room temperature MS of Fe–Al alloys[14] shows similar compositional dependence to Fe–Ga alloys; it increases with Al content in the A2 phase region, reaching a maximum at around 20 at. % Al (near the phase boundary[13]) and then decreases with Al content in the $A2+D0_3$ two phases region. Unlike Fe–Ga, MS in the aluminum alloys continues to a decrease in the $D0_3$ single phase region, consistent with the rapidly decreasing Curie temperature and loss of ferromagnetism at ~30 at. % Al.[15] In addition, Fe–Al alloys respond to thermal treatments differently from Fe–Ga alloys;[14] usually water quenched Fe–Ga (Ref. 3) and Fe–Ga–C (Ref. 8) alloys have higher magnetostriction than slow cooled ordered ones and this effect is most dramatic near the phase boundary and is attributed to the prevention of $D0_3$ formation during quenching,[8] whereas the water quenched Fe–Al alloys have a slightly lower MS than those of slow cooled ones when Al content is >15 at. %.[16] The origin of these differences was not clear. In this work, we examined the influence of C on MS of alloys in the Fe–Al system to assess whether carbon has a similar effect in Fe–Al as was found in Fe–Ga alloys and whether this would provide insight in the thermal behavior differences in the binary alloys.

II. EXPERIMENTS

Appropriate quantities of electrolytic grade iron (99.99% purity) contained the following major impurities in ppm (weight) C~10 and O~60, electronic grade gallium (99.9999% purity), and electronic grade aluminum (99.99%

a)Electronic mail: mhuang@ameslab.gov.

purity) were arc melted several times into buttons under an argon atmosphere. Carbon additions of 400 ppm by weight were made using arc melted Fe–5 at. % C master alloys. The buttons were then remelted and the alloy drop cast into a copper chill cast mold to ensure compositional homogeneity throughout the ingot. Single crystal growth was done using the Bridgman technique in a resistance furnace. Following crystal preparation, the ingots were annealed at 1000 °C for 168 h to homogenize the composition and were cooled at 10 °C/min in a furnace filled with high purity argon. Oriented (100) disks, 6 mm in diameter and 2–3 mm thick, were sectioned from the ingot and marked with in-plane [100] and [110] directions for strain gage alignment. MS was measured by rotating the disk in a 20 kOe magnetic field applied parallel to the face of the disk. The resulting strain was fitted to the lowest order MS term which follows a $\cos^2\theta$ angular dependence. The next higher order MS term, which follows a $\cos^4\theta$ angular dependence, was generally found to be less than 10 ppm. MS was also measured on the disks after annealing in a sealed quartz tube at 1000 °C for 4 h and quenched into water. Fe–Al–C alloys were wrapped with tantalum foil to prevent the reaction between aluminum and the quartz tube.

Composition measurements of each disk were done by energy-dispersive spectrometry in a JEOL 840A scanning electron microscope using Fe–Ga and Fe–Al alloys with known composition as internal standards. The composition was determined by the average of five measurements evenly distributed across the disk. Carbon content was analyzed using combustion gas analyzer method and about 0.5 g of alloys was used for each sample.

Powders for x-ray diffraction (XRD) were made by filing the ingot, followed by annealing at 600 °C in a sealed quartz tube filled with high purity Ar to release the residual stress. XRD studies were conducted in a Panalytical X'Pert diffractometer with Cu $K\alpha$ radiation at 45 kV and 40 mA. The scans were performed over a 2θ range of 20°–90° using a scan step of 0.02°.

High-energy transmission x-ray experiments were performed at Sector-6 Advance Phonon Source. Monochromatic x-ray of 100 keV was used. The sample size was $5\times5\times0.5$ mm^3. Oriented samples were prepared using standard metallographic procedures with the final polishing step using 1 μm diamond paste, followed by a light Nital etch. The last step was found to be crucial in the removal of surface damage layers, thereby eliminating the formation of diffuse Debye rings observed at the positions of the primary reflections of the cubic phases.

III. RESULTS

The MS for Fe–Ga–C and Fe–Al–C alloys is summarized in Table I. The MS and structural characterization of Fe–Ga–C alloys containing up to ~30 at. % Ga are presented first, followed by the MS of Fe–Al–C alloys up to ~25 at. % Al. The results of the MS are classified by and described in the categories of slow cooled and quenched samples. The MS of Fe–Ga–C and Fe–Al–C alloys is generally higher than that of Fe–Ga (Ref. 11) and Fe–Al (Refs. 14 and 16) binary alloys and followed a similar trend of the binary alloys.

TABLE I. MS of Fe–Ga–C and Fe–Al–C alloys.

	$3/2\ \lambda_{100}$ (ppm)	
Composition	Slow cooled	Water quenched
$Fe_{90.14}Ga_{9.7}C_{0.16}$ [a]	152	147
$Fe_{87.84}Ga_{11.9}C_{0.16}$ [a]	202	204
$Fe_{83.78}Ga_{16.0}C_{0.22}$	326	310
$Fe_{83.7}Ga_{16.2}C_{0.08}$ [b]	268	279
$Fe_{82.4}Ga_{17.6}C_{0.07}$ [b]	322	298
$Fe_{81.4}Ga_{18.6}C_{0.08}$ [b]	369	334
$Fe_{81.3}Ga_{18.6}C_{0.17}$ [a]	342	369
$Fe_{80.38}Ga_{19.6}C_{0.03}$ [a]	311	396
$Fe_{78.92}Ga_{20.9}C_{0.18}$ [a]	307	432
$Fe_{77.1}Ga_{22.7}C_{0.20}$ [a]	258	317
$Fe_{75.21}Ga_{24.3}C_{0.49}$ [a]	251	310
$Fe_{73.2}Ga_{26.7}C_{0.10}$	169	450
$Fe_{72.59}Ga_{27.3}C_{0.11}$	131	125
$Fe_{72.17}Ga_{27.7}C_{0.13}$	113	141
$Fe_{71.76}Ga_{28.1}C_{0.14}$	110	169
$Fe_{86.57}Al_{13.4}C_{0.03}$	158	158
$Fe_{82.74}Al_{17.2}C_{0.06}$	199	201
$Fe_{81.24}Al_{18.56}C_{0.19}$	204	192
$Fe_{77.96}Al_{22}C_{0.04}$	165	156
$Fe_{77.40}Al_{22.5}C_{0.10}$	145	124
$Fe_{76.37}Al_{23.5}C_{0.13}$	130	122

[a]Data published in Ref. 8.
[b]Data published in Ref. 9.

A. Fe–Ga–C alloys

1. Fe–Ga–C alloys with ~10–27 at. % Ga

It can be seen from Fig. 1 that the MS of the water quenched ternary Fe–Ga–C alloys followed a similar trend as that of the quenched Fe–Ga binary alloys,[11] i.e., a two-peak curve that has shifted in the following way: the MS is generally higher in the ternary through the second peak with a gallium content of up to ~27 at. %; the first peak with a value of 432 ppm is about 10% higher than that in the binary with a value of 397 ppm and shifted to a higher gallium composition; and the second peak is also higher but shifted

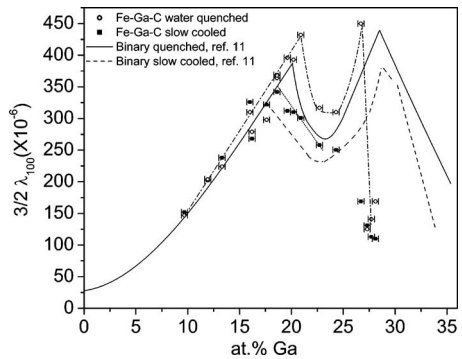

FIG. 1. MS of Fe–Ga–C alloys in the slow cooled and water quenched states compared with that of the binary Fe–Ga alloys. Trend lines are drawn to guide eyes.

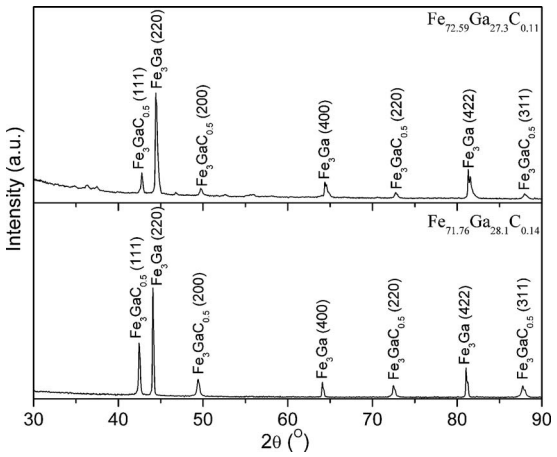

FIG. 2. XRD patterns show a mixture of $Fe_3GaC_{0.5}$ and Fe_3Ga ($D0_3$) phases in the $Fe_{72.59}Ga_{27.3}C_{0.11}$ and $Fe_{71.76}Ga_{28.1}C_{0.14}$ alloys.

to a lower gallium composition. A maximum of 450 ppm was obtained for the alloy with 26.7 at. % Ga, which is the highest value reported so far for iron-based alloys and is higher than that in the binary alloy with a MS of 440 ppm at 28.5 at. % Ga. It should be noted that these are preliminary data and further studies with controlled carbon additions are needed to confirm the trend for the second peak.

The MS of the slow cooled Fe–Ga–C alloys with 10–24.5 at. % Ga also follows a similar trend as in the binary alloys,[11] and like that of the quenched samples, is generally higher than the MS of the binary alloys with a similar Ga content. MS increases with gallium content in the A2 region and reaches a maximum of 369 ppm at 18.6 at. % Ga, about 16% higher than the peak value of 319 ppm at 17.9 at. % Ga for the binary alloys and then decreases in the $A2+D0_3$ region.

2. Fe–Ga–C alloys with ~27–30 at. % Ga

It can be seen from Fig. 1 that the MS of both slow cooled and water quenched Fe–Ga–C alloys with ~27–30 at. % Ga is much lower than that of the binary Fe-Ga alloys with similar gallium contents. The MS is comparable to that of Fe–Ga alloys with ~30–35 at. % Ga, in which a second phase Fe_6Ga_5 was found. Powder XRD was used to investigate whether the decrease in MS of the Fe–Ga–C alloys with ~27–30 at. % Ga is also related to the formation of a similar second phase (Fe_6Ga_5) as in the binary alloys. The result shown in Fig. 2 indicates there are two phases in the alloys. One phase can be indexed as $Fe_3GaC_{0.5}$ (Ref. 17) carbide with a perovskite structure.[18] It can be considered as an ordered face-centered-cubic (fcc) arrangement of Fe and Ga of type $L1_2$ with carbon atoms in the octahedral interstices. The other phase might be $D0_3$ phase though only peaks corresponding to a disordered bcc (A2) structure were found because of the similar atomic scattering factors of Fe and Ga atoms precludes the detection of the superlattice peaks on the powder sample. In order to clarify whether the other phase is A2 or $D0_3$, high-energy synchrotron x-ray was used to investigate the structure of Fe–26.7 at. % Ga–C single crystal. This alloy was chosen because when quenched it has the highest MS and largest difference in MS between

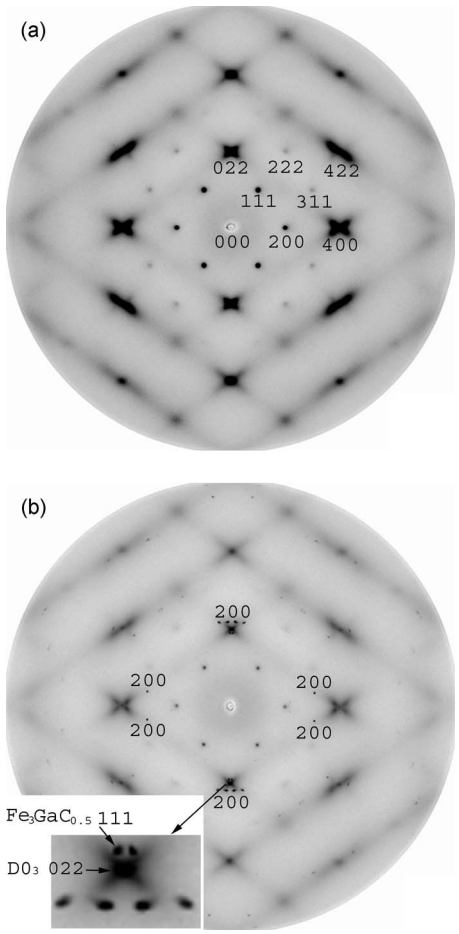

FIG. 3. Synchrotron x-ray results of Fe–26.7 at. %Ga–C alloy show the $D0_3$ structure in both water quenched (a) and slow cooled (b) samples. The indexed spots in slow cooled sample (b) are from the (200) plane of the $Fe_3GaC_{0.5}$ carbide; the enlarged portion shows the epitaxial relationship between the (022) plane of $D0_3$ and (111) and (200) planes of $Fe_3GaC_{0.5}$.

the water quenched and slow cooled conditions. Figure 3 shows high-energy synchrotron x-ray patterns for Fe–26.7 at. % Ga–C single crystal in the [011] zone axis. The appearance of superlattice spots at (111) and (200) planes indicates the existence of the $D0_3$ phase in both slow cooled and water quenched alloys. There are additional spots close to the (022) spot in the pattern for the slow cooled alloy [Fig. 3(b)], which could be related to $Fe_3GaC_{0.5}$ phase shown in Fig. 2. It can be seen from the XRD pattern shown in Fig. 2 that the d-spacing for (111) and (200) planes in $Fe_3GaC_{0.5}$ is very close to that of (022) plane in $D0_3$ phase and the mismatch between (022) plane of $D0_3$ and (111) and (200) planes of $Fe_3GaC_{0.5}$ is about 3% and 10%, respectively. The small mismatch makes it possible that the (111) and (200) plane of the $Fe_3GaC_{0.5}$ carbide grows epitaxial on the (022) plane of the $D0_3$ phase as shown in the enlarged portion in Fig. 3(b). It can be seen from Fig. 3(a) that, except for the diffraction pattern of $D0_3$, no extra spots were found in the pattern for the water quenched alloy, indicating that the carbide was dissolved into the matrix by high temperature annealing and the solubility of carbon in this alloy is higher at elevated temperature. As a result of retaining a single phase, the MS increased in the water quenched alloys. This is consistent with binary alloys where a second phase usually results in decreased MS.[11]

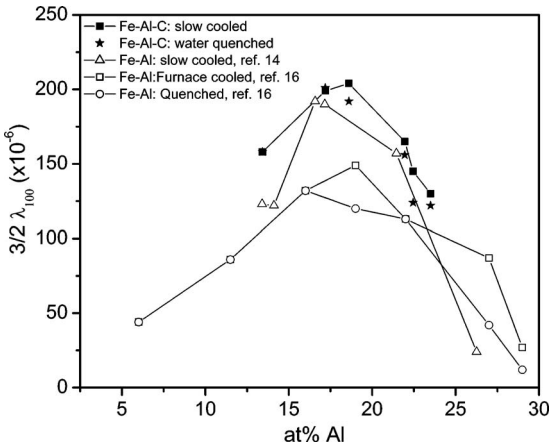

FIG. 4. MS of Fe–Al–C alloys compared with the binary Fe–Al alloys.

3. Comparison between slow cooled and quenched alloys

The effect of quenching on MS for Fe–Ga–C alloys is different in different phase regions, which is similar to Fe–Ga binary alloys. It can be seen that, in the A2 region with gallium content less than 18.6 at. % Ga, the MS of the water quenched alloys is equal to or slightly lower than that of the slow cooled alloys, indicating that quenching does not help in improving the MS in this composition range. However, a significant increase in MS by quenching from high temperature was observed for almost all of the alloys with gallium content beyond 18.6 at. % Ga. Largest improvement in MS by quenching was observed near the phase boundary. For example, the MS increased from 301 to 432 ppm for the Fe–20.9 at. % Ga–C alloy and from 169 to 450 ppm for the Fe–26.7 at. % Ga–C alloy, increases of 43% and 165%, respectively.

B. Fe–Al–C alloys

Figure 4 shows the MS of Fe–Al–C alloys together with the Fe–Al binary alloys.[14,16] The MS of the carbon-doped alloys are compositionally dependent with a trend that is similar to the binary Fe–Al alloys; it increases with Al content and reaches a maximum with a value of 204 ppm at around 18.6 at. % Al (near the solubility limit) and then decreases. It can also be seen that the additions of small amounts of C (0.03–0.19 at. %) increases the MS over the binary alloys. The measured MS for the Fe–Al–C alloys in this study is about 30%–45% higher than that of binary Fe–Al alloys reported by Hall[16] and is about 5%–30% higher than the result for Fe–Al binary alloys in our previous study.[14] For Fe–Al–C alloys with $<\sim 18$ at. % Al in the A2 region, the MS of water quenched alloys is equal to that of slow cooled samples, whereas for alloys with >18 at. % Al in the A2+$D0_3$ or $D0_3$ phase region, the MS of the water quenched Fe–Al–C alloys is slightly lower than that in the slow cooled condition. Similar quenching effect for the binary alloys was reported by Hall.[16]

IV. DISCUSSION

The addition of carbon into Fe–Al and Fe–Ga generally increased the MS in the whole composition range for these two systems except for the region where $Fe_3GaC_{0.5}$ formed in Fe–Ga–C. This is different from the addition of transition metals, which generally shows a reduction in the MS of Fe–Ga alloys.[9] The different effects on the MS by the addition of transition metals and carbon is believed to result from their occupation site within the crystal lattice. It is reasonable to believe that small atoms such as carbon enter into the octahedral site as they do in pure α-iron.[19–22] In fact, since the lattice parameters for the A2 phase increases with the concentration of substitutional solute atoms such as Al (Refs. 13 and 23) and Ga,[24] this will, in turn, increase the radius of octahedral site across the entire composition range, thereby further favoring the octahedral site preferentially. Though the alloying of Al or Ga into pure α-iron could lead to the creation of energetically favorable but different positions for carbon atoms in the bcc Fe lattice, carbon atoms were reported to occupy the octahedral site in both A2 and $D0_3$ in Fe–Al (Ref. 25), which is consistent with the current result. Considering the similarity of Fe–Al (Ref. 13) and Fe–Ga (Refs. 12 and 13) systems, it is reasonable to believe that carbon atoms remain on the octahedral site in both systems. Further, since carbon is larger than the available octahedral site in α-iron, carbon is known to produce a tetragonal distortion,[19] and by analogy, Fe–Ga and Fe–Al alloys will also be tetragonally distorted. Ga pairing along the $\langle 100 \rangle$ directions is thought to contribute to the enhanced magnetoelasticity of Fe–Ga alloys[5] and this pairing is accompanied by tetragonal distortions crystallographically equivalent to carbon occupying the octahedral site.

The addition of carbon also changes the solubility limit of Ga in both the A2 and $D0_3$ phase regions. It is known that for the slow cooled Fe–Ga alloys,[11] the MS reaches a maximum at 17.9 at. % Ga and this composition corresponds to the solubility limit of Ga in the A2 phase. With carbon present and for the same slow cooled conditions, the maximum MS of 369 ppm occurs at a composition around 18.6 at. % Ga, which we interpret as the solubility limit of Ga in the A2 phase when trace levels of carbon are present. A similar result is found for water quenched alloys, where a maximum MS (432 ppm) is observed at higher gallium composition than that in quenched binary alloys ($\sim$390 ppm). In contrast to the A2 phase, the addition of carbon to $D0_3$ phase narrows the solubility range with respect to Ga. The MS of Fe–Ga–C alloys in the $D0_3$ phase region reaches a maximum of 450 ppm at 26.7 at. % Ga, whereas the maximum MS of the binary alloys reaches 440 ppm at 28.5 at. % Ga. Again using the fact that the maximum in MS occurs at the edge of the phase field and is correlated with the formation of a second phase, the maximum in MS suggests that for water quenched carbon-doped $D0_3$ phase the solubility limit decreases relative to the binary system. This effect of the added carbon on the solubility in A2 and $D0_3$ phase regions is clearly indicated in the MS of Fe–Ga–C alloys, as shown in Fig. 1, the U-shaped trend line occurring over a much narrower composition range for water quenched Fe–Ga–C al-

loys. No phase diagram for the Fe–Ga–C is available to directly support this conclusion. However, with Al and Ga being in the same group of the Periodic Table and the similarity in the binary Fe–Al (Ref. 13) and Fe–Ga,[12] the Fe–Al–C system is likely representative of the phase equilibria of Fe–Ga–C. Three isotherms at 800, 1000, and 1200 °C have been published for the Fe–Al–C system.[26] Fe–Ga–C alloys in this study were water quenched from 1000 °C; therefore, the 1000 °C isotherm is particular relevant to the water quenched conditions. From this isotherm, it can be clearly seen that the phase boundary for the A2 phase is pushed to higher Al content by the addition of carbon,[26] which is consistent with the present result that the MS for the Fe–Ga–C alloys peaked at a higher Ga concentration than the binary alloys in the A2 region.

The dramatic decrease in the MS for the Fe–Ga–C alloys with ~26–30 at. % Ga is due to the appearance of $Fe_3GaC_{0.5}$ carbide. It is known that the existence of a second phase decreases the MS of Fe–Ga alloys.[11] This is also true for the Fe–Ga–C ternary alloys. For binary alloys, the drastic decrease in MS beyond the $D0_3$ single phase region is due to the formation of Fe_6Ga_5.[11] The formation of Fe_6Ga_5 could also be the reason for the decrease in MS for the Fe–Ga–C alloys. However, $Fe_3GaC_{0.5}$ carbide was not found in the water quenched but in the slow cooled Fe–26.7 at. % Ga–C alloy and, accordingly, the MS dropped from 450 to 169 ppm, indicating that $Fe_3GaC_{0.5}$ carbide is most likely the reason for the dramatic decrease in MS in this composition range. The phase fraction of the carbide increased with carbon content and much more carbide was found in crystals with higher carbon content, as shown in Fig. 2. This large amount of carbide cannot be dissolved completely by high temperature annealing, followed by water quench. As a result, though the MS of the water quenched Fe–Ga–C alloys with ~27–30 at. % Ga is higher than that of the slow cooled samples with the same Ga concentration, they are both much lower than that of the binary alloys.

It can be seen in Table I that there is a significant variation in the carbon content. This variation results from inconsistent melt practices as well as reaction of the carbon with trace oxygen in the starting materials. Coupled with the inherent macrosegregation of gallium along the length of the crystal during crystal growth by the Bridgman method, the actual variation in MS at a fixed Ga composition is difficult to achieve in practice. Clearly, systematic control of carbon (as well as Ga) would lead to a better understanding of the effect of carbon on MS.

The MS of the water quenched Fe–Al–C alloys in the A2 region (up to ~18 at. % Al) is equal to or slightly higher than that of the slow cooled alloys, which is similar to the Fe–Ga–C alloys in the A2 region. However, unlike Fe–Ga–C alloys, improvement in MS by quenching was not found for the Fe–Al–C alloys near the A2 and $D0_3$ phase boundaries. In contrast, the MS in the water quenched Fe–Al–C alloys with ~18–25 at. % Al is slightly lower than that of the slow cooled ones. Similar results were reported by Hall that quenching decreased the MS in Fe–Al alloys.[16] The different response to the thermal treatment for the Fe–Ga–C and Fe–Al–C alloys could be due to the phase transition in these two systems. Our previous study showed that water quenching can keep the A2 phase and prevent the formation of $D0_3$ phase near the A2 phase boundary in the Fe–Ga (Refs. 3 and 27) and Fe–Ga–C (Ref. 8) systems. In contrast, water quench does not fully retain the disordered A2 phase in the Fe–Al system. For example, a disordering anneal, followed by a rapid quenching of an Fe–23 at. % Al alloy into cold brine did not completely suppressed the FeAl ordering and a fine ordered FeAl (B2) phase was found embedded in the disordered A2 matrix.[28] The B2 ordered phase will transform into Fe_3Al ($D0_3$) by slow cooling.[29] While the $D0_3$ phase is ferromagnetic at room temperature, the ordered B2 is paramagnetic.[13] They respond to the magnetic field differently. This could explain why there is no improvement in MS for water quenched Fe–Al–C alloys with ~18–25 at. % Al and is consistent with our previous study in binary Fe–Al.[14]

V. CONCLUSION

In summary, we have investigated the effect of carbon addition on the MS of Fe–Ga and Fe–Al alloys. The added carbon generally increased the MS for the alloys in the Fe–Ga and Fe–Al systems. The carbon addition also changed the solubility limit of the A2 and $D0_3$ phases. The formation of carbide in the Fe–Ga–C alloys with a composition near the $D0_3$ phase region is detrimental to the MS. Fe–Al–C and Fe–Ga–C alloys behaved differently upon quenching. The MS in the quenched Fe–Al–C alloys is equal to or slightly lower than that of the slow cooled ones, whereas the MS is generally higher in quenched Fe–Ga–C alloys than slow cooled ones especially in the region near the A2 or $D0_3$ phase boundaries.

ACKNOWLEDGMENTS

This work was supported by the Office of Naval Research under ONR MURI Contract No. N000140610530. The research was performed at the Ames Laboratory. Ames Laboratory is operated for the U.S. Department of Energy by Iowa State University under Contract No. DE-AC02-07CH11358.

[1] A. E. Clark, J. B. Restorff, M. Wun-Fogle, T. A. Lograsso, and D. L. Schlagel, IEEE Trans. Magn. **36**, 3238 (2000).
[2] A. E. Clark, M. Wun-Fogle, J. B. Restorff, and T. A. Lograsso, Mater. Trans. **43**, 881 (2002).
[3] A. E. Clark, M. Wun-Fogle, J. B. Restorff, T. A. Lograsso, and J. R. Cullen, IEEE Trans. Magn. **37**, 2678 (2001).
[4] A. E. Clark, K. B. Hathaway, M. Wun-Fogle, J. B. Restorff, T. A. Lograsso, V. M. Keppens, G. Petculescu, and R. A. Taylor, J. Appl. Phys. **93**, 8621 (2003).
[5] J. R. Cullen, A. E. Clark, M. Wun-Fogle, J. B. Restorff, and T. A. Lograsso, J. Magn. Magn. Mater. **226–230**, 948 (2001).
[6] T. A. Lograsso, A. R. Ross, D. L. Schlagel, A. E. Clark, and M. Wun-Fogle, J. Alloys Compd. **350**, 95 (2003).
[7] G. Petculescu, K. B. Hathaway, T. A. Lograsso, M. Wun-Fogle, and A. E. Clark, J. Appl. Phys. **97**, 10M315 (2005).
[8] M. Huang, T. A. Lograsso, A. E. Clark, J. B. Restorff, and M. Wun-Fogle, J. Appl. Phys. **103**, 07B314 (2008).
[9] A. E. Clark, J. B. Restorff, M. Wun-Fogle, K. B. Hathaway, T. A. Lograsso, M. Huang, and E. Summers, J. Appl. Phys. **101**, 09C507 (2007).
[10] N. Kawamiya and K. Adachi, J. Magn. Magn. Mater. **31–34**, 145 (1983).
[11] Q. Xing, Y. Du, R. J. McQueeney, and T. A. Lograsso, Acta Mater. **56**, 4536 (2008).
[12] O. Ikeda, R. Kainuma, I. Ohnuma, K. Fukamichi, and K. Ishida, J. Alloys

Compd. **347**, 198 (2002).
[13]H. Okamoto, in *Phase Diagrams of Binary Iron Alloys*, edited by H. Okamoto (ASM International, Materials Park, OH, 1993).
[14]A. E. Clark, J. B. Restorff, M. Wun-Fogle, D. Wu, and T. A. Lograsso, J. Appl. Phys. **103**, 07B310 (2008).
[15]P. Shukla and M. Wortis, Phys. Rev. B **21**, 159 (1980).
[16]R. C. Hall, J. Appl. Phys. **30**, 816 (1959).
[17]PDF File No. 01-089-7274.
[18]H. H. Stadelmaier, L. J. Huetter, and N. C. Kothari, Z. Metallkd. **51**, 41 (1960).
[19]G. K. Williamson and R. E. Smallman, Acta Crystallogr. **6**, 361 (1953).
[20]R. R. Hasiguti and G. Kamoshita, J. Phys. Soc. Jpn. **9**, 646 (1954).
[21]W. R. Thomas and G. M. Leak, Nature (London) **176**, 29 (1955).
[22]M. E. Hermant, Acta Metall. **16**, 1 (1968).
[23]A. Taylor and R. M. Jones, Phys. Chem. Solids **6**, 16 (1958).
[24]J. M. Borrego, J. S. Blazquez, C. F. Conde, A. Conde, and S. Roth, Intermetallics **15**, 193 (2007).
[25]I. S. Golovin, M. S. Blanter, T. V. Pozdova, K. Tanaka, and L. B. Magalas, Phys. Status Solidi A **168**, 403 (1998).
[26]M. Palm and G. Inden, Intermetallics **3**, 443 (1995).
[27]S. Datta, M. Huang, J. Raim, T. A. Lograsso, and A. B. Flatau, Mater. Sci. Eng., A **A435–A436**, 221 (2006).
[28]S. M. Allen and J. W. Cahn, Acta Metall. **24**, 425 (1976).
[29]O. Ikeda, I. Ohnuma, R. Kainuma, and K. Ishida, Intermetallics **9**, 755 (2001).